Check for updates

Chaos and Complexity in Engineering - Research Article

Advances in Mechanical Engineering

Advances in Mechanical Engineering
2019, Vol. 11(5) 1–11
© The Author(s) 2019
DOI: 10.1177/1687814019851004
journals.sagepub.com/home/ade
SAGE

Nonlinear forced vibration of a moving paper web with varying density

Mingyue Shao[1,2], Jimei Wu[1,2], Yan Wang[3], Qiumin Wu[1] and Shudi Ying[2]

Abstract

The study investigates the forced nonlinear vibration characteristics of an axially moving printing paper web with variable density in the lateral direction. The nonlinear governing equations of the web can be obtained by the von Karman large deflection thin plate theory. The vibration equations are discretized using the Bubnov–Galerkin method. The fourth-order Runge–Kutta technique is used to solve the differential equations of the nonlinear system. The phase-plane diagrams, time histories, bifurcation graphs, Poincare maps, and power spectrum are employed to analyze the influence of density coefficient, velocity, and aspect ratio on the nonlinear dynamic behavior of the moving paper web. The stable working region and the divergence instability region of the web are obtained. The research provides a theoretical foundation for improving the dynamic stability of a moving paper web.

Keywords

Nonlinear forced vibration, variable density, moving paper web, fourth-order Runge–Kutta technique

Date received: 27 September 2018; accepted: 23 April 2019

Handling Editor: James Baldwin

Introduction

In printing, the surface density of a printing web corresponding to each printout is different. In addition, the ink and fountain solution used during the printing process will affect the density of the web surface, and the uneven thickness of the substrate will change surface density, the vibration characteristics of printing webs will change, and in this manner, the web is prone to wrinkling, tearing, and surface scratches; as a result, the overprint accuracy and printing quality will reduce.[1] Therefore, it is important to investigate the nonlinear vibration characteristics of a web with variable density.

The axially moving systems include plates, beams, strings, and webs. Many scholars have studied the dynamics of axially moving systems. Specifically, mathematical modeling, solution methods, parameter vibrations, external excitation systems, elastic supports, and different boundary conditions are mainly analyzed in axially moving systems. Mote[2] first discussed the nonlinear vibration problem of axially moving strings, and the effect of axial velocity on vibration was emphasized. Wickert and Mote[3] then studied the response of moving loads on moving strings. Pakdemirli et al.[4] studied the transverse vibration of axially accelerated strings. The equation was established based on Hamilton's principle, and the Galerkin method was applied to discretize partial differential equation. The Floquet theory was used to analyze the stability of

[1]Faculty of Printing, Packaging and Digital Media Engineering, Xi'an University of Technology, Xi'an, China
[2]Faculty of Mechanical and Precision Instrument Engineering, Xi'an University of Technology, Xi'an, China
[3]Faculty of Civil Engineering and Architecture, Xi'an University of Technology, Xi'an, China

Corresponding author:
Jimei Wu, Faculty of Printing, Packaging and Digital Media Engineering, Xi'an University of Technology, Xi'an 710048, China.
Email: wujimei1@163.com

Creative Commons CC BY: This article is distributed under the terms of the Creative Commons Attribution 4.0 License (http://www.creativecommons.org/licenses/by/4.0/) which permits any use, reproduction and distribution of the work without further permission provided the original work is attributed as specified on the SAGE and Open Access pages (https://us.sagepub.com/en-us/nam/open-access-at-sage).

strings. Chen et al.[5–7] systematically studied the nonlinear vibration characteristics of axially moving viscoelastic strings based on the fourth-order Galerkin truncation and the method of multiple scales. The effects of average speed, speed, and speed variation frequency on system stability were analyzed. Kesimli et al.[8] analyzed the characteristics of nonlinear vibration of a multi-supported axially moving string. Pellicano and Vestroni[9] investigated the nonlinear dynamics of simply supported beams, bifurcation, and stability analysis on the subcritical and supercritical velocity ranges. Öz et al.[10] applied the method of multiple scales to study the nonlinear vibration characteristics of axially moving beams. Ghayesh and colleagues[11–13] systematically studied the nonlinear dynamics of beams with variable velocity and intermediate elastic support, and the nonlinear resonance response and global dynamics of the system at subcritical velocity were also studied. Tang et al.[14] studied the nonlinear steady-state oscillation response of axially accelerated viscoelastic beams by the method of multiple scales. Yang et al.[15] applied the finite element method to study the linear free vibration and nonlinear forced vibration of axially moving viscoelastic plates. Wang et al.[16] studied the dynamic characteristics and stability of a paperboard with elastic point support and elastic edge constraint. The extended Hamilton principle was used to establish the equation of the system, and the meshless Galerkin method was used to discretize equation. The critical speeds were obtained in different conditions. Wang and Zu[17] analyzed the effects of some key parameters on nonlinear behaviors of functionally graded rectangular plates with porosities and moving in thermal environment using the method of harmonic balance. Marynowski[18,19] applied the Galerkin method and the fourth-order Runge–Kutta technique to analyze nonlinear vibration and stability of an axially moving paper web. Lin and Mote[20] investigated the nonlinear vibration of a web with little bending stiffness and subjected to a transverse load. Zhao and Wang[21] analyzed the large deflection vibration of a web by the Galerkin method and the differential quadrature method. Soares and Gonçalves[22] examined the nonlinear vibration of a pre-stretched hyper-elastic annular web under finite deformations by the shooting method and the finite element method. Gajbhiye et al.[23] studied the large deflection vibration of a rectangular, flat thin membrane using finite element method. Li et al.[24] investigated the stochastic dynamic response and reliability analysis of orthotropic membrane structures under impact loading by the perturbation method. In addition, the influence of parameters such as impact velocity, preload, and radius on structural reliability was also analyzed.

Recently, there have been many publications dealing with the linear vibration of the membrane with variable density, but few publications about the forced nonlinear vibration characteristics of a printing web with variable density. Jabareen and Eisenberger[25] investigated the transverse vibration of a non-homogeneous membrane with variable density by the dynamic stiffness method. Subrahmanyam and Sujith[26] analyzed the perpendicular movements resulting in vibration of annular membranes with continuously variable density. Willatzen[27] established a general quasi-analytical model based on the Frobenius power series expansion method to analyze the vibration of solid circular and annular membranes with continuously varying density. Ma et al.[28] studied the vibration control of the moving web with variable density by the sub-optimal control method. Buchanan[29] analyzed the stability of the circular membrane with linear variation density in the diameter direction.

In the following research, the nonlinear vibration and stability of the moving printing paper web with variable density in the lateral direction based on von Karman large deflection thin plate theory are investigated. The fourth-order Runge–Kutta technique is adopted to solve the differential equations, and the effects of the density coefficient, aspect ratio, and moving speed on the nonlinear vibration of an axially moving web with variable density are analyzed.

Establishment of vibration model of a variable density web

Figure 1 shows the principle model of a moving paper web; the web is soft and has no bending stiffness. The web moves in the x-direction with a moving speed of v; the width direction of the web is in the y-direction; and the transverse vibration direction is in the z-direction. Supposing $\bar{w}(x, y, t)$ represents the displacement of transverse vibration of the web, and T_x and T_y denote the pulling or dragging force acting along unit length of web at the boundaries in x and y directions, separately; a is the web length; b is the web width; $\bar{p}\cos\bar{\omega}t$ denotes the in-plane uniform external excitation; and $\bar{p}$ denotes the amplitude of external excitation. Figure 2 shows the law of a moving web with a variable density in the lateral direction; the initial value of the surface density and density coefficient is ρ_0 and α, respectively.

Equilibrium differential equations can be defined as[30]

$$\begin{cases} \dfrac{\partial N_x}{\partial x} + \dfrac{\partial N_{xy}}{\partial y} = 0 \\ \dfrac{\partial N_y}{\partial y} + \dfrac{\partial N_{yx}}{\partial x} = 0 \end{cases} \tag{1}$$

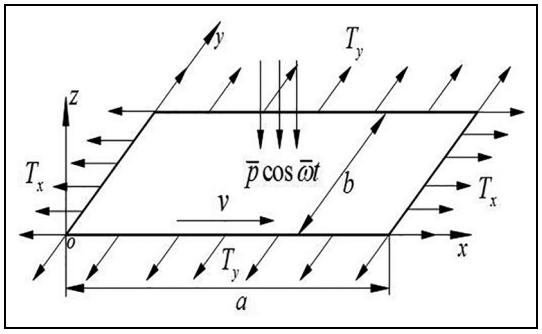

Figure 1. Mechanical model of the axially moving web.

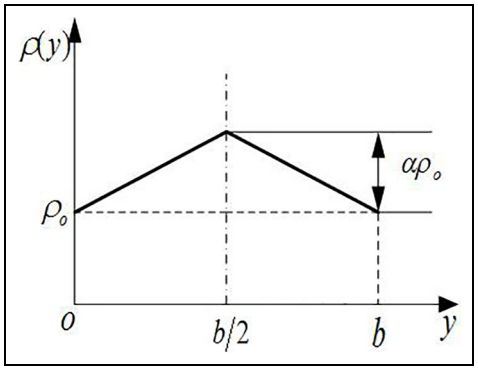

Figure 2. Law of a moving web with varying density.

Elastic surface differential equation is expressed as

$$\rho\left(\frac{\partial^2\overline{w}}{\partial t^2}+2v\frac{\partial^2\overline{w}}{\partial x\partial t}+v^2\frac{\partial^2\overline{w}}{\partial x^2}\right)-N_x\frac{\partial^2\overline{w}}{\partial x^2}-N_y\frac{\partial^2\overline{w}}{\partial y^2}-2N_{xy}\frac{\partial^2\overline{w}}{\partial x\partial y}+\lambda\frac{\partial\bar{w}}{\partial t}=\bar{p}\cos\bar{\omega}t \tag{2}$$

where N_x, N_y, and N_{xy} denote the web inner forces per unit length and λ is the damping coefficient.

The system compatibility equation is expressed as

$$\frac{\partial^2 N_x}{\partial y^2}+\frac{\partial^2 N_y}{\partial x^2}-\mu\frac{\partial^2 N_x}{\partial x^2}-\mu\frac{\partial^2 N_y}{\partial y^2}-2(1+\mu)\frac{\partial^2 N_{xy}}{\partial x\partial y}=Eh\left[\left(\frac{\partial^2\bar{w}}{\partial x\partial y}\right)^2-\frac{\partial^2\bar{w}}{\partial x^2}\frac{\partial^2\bar{w}}{\partial y^2}\right] \tag{3}$$

where μ denotes Poisson's ratio of the web, E denotes the elastic modulus of the web, and h is the thickness of the web.

The inner force function of the paper web is expressed as

$$N_x=\frac{\partial^2\varphi}{\partial y^2},\quad N_y=\frac{\partial^2\varphi}{\partial x^2},\quad N_{xy}=-\frac{\partial^2\varphi}{\partial x\partial y} \tag{4}$$

where ϕ corresponds to the internal force function.

The web units are independent from each other, so the following is obtained

$$N_x\big|_{x=0,a}=T_x\qquad N_y\big|_{y=0,b}=T_y\qquad N_{xy}=0 \tag{5}$$

According to von Karman large deflection thin plate theory,[30] the nonlinear forced vibration equations can be stated as follows

$$\rho(y)\left(\frac{\partial^2\bar{w}}{\partial t^2}+2v\frac{\partial^2\bar{w}}{\partial x\partial t}+v^2\frac{\partial^2\bar{w}}{\partial x^2}\right)-\frac{\partial^2\varphi}{\partial y^2}\frac{\partial^2\bar{w}}{\partial x^2}-\frac{\partial^2\varphi}{\partial x^2}\frac{\partial^2\bar{w}}{\partial y^2}+\lambda\frac{\partial\bar{w}}{\partial t}=\bar{p}\cos\bar{\omega}t \tag{6a}$$

$$\frac{\partial^4\varphi}{\partial x^4}+\frac{\partial^4\varphi}{\partial y^4}=Eh\left[\left(\frac{\partial^2\bar{w}}{\partial x\partial y}\right)^2-\frac{\partial^2\bar{w}}{\partial x^2}\frac{\partial^2\bar{w}}{\partial y^2}\right] \tag{6b}$$

The density function $\rho(y)$ can be denoted as

$$\rho(y)=\begin{cases}\rho_0\left(1+2\alpha\frac{y}{b}\right) & \left(0\leqslant y\leqslant\frac{b}{2}\right)\\ \rho_0\left(1+2\alpha-2\alpha\frac{y}{b}\right) & \left(\frac{b}{2}\leqslant y\leqslant b\right)\end{cases} \tag{7}$$

Another form of $\rho(y)$ is

$$\rho(y)=\rho_0(1+\alpha)-2\alpha\rho_0\left|\frac{y}{b}-\frac{1}{2}\right| \tag{8}$$

Equation (8) is substituted into equation (6) to obtain the nonlinear forced vibration equations of the moving paper web with variable density

$$\left[(1+\alpha)\rho_0-2\alpha\rho_0\left|\frac{y}{b}-\frac{1}{2}\right|\right]\left(\frac{\partial^2\bar{w}}{\partial t^2}+2v\frac{\partial^2\bar{w}}{\partial x\partial t}+v^2\frac{\partial^2\bar{w}}{\partial x^2}\right)-\frac{\partial^2\varphi}{\partial y^2}\frac{\partial^2\bar{w}}{\partial x^2}-\frac{\partial^2\varphi}{\partial x^2}\frac{\partial^2\bar{w}}{\partial y^2}+\lambda\frac{\partial\bar{w}}{\partial t}=\bar{p}\cos\bar{\omega}t \tag{9a}$$

$$\frac{\partial^4\varphi}{\partial x^4}+\frac{\partial^4\varphi}{\partial y^4}=Eh\left[\left(\frac{\partial^2\bar{w}}{\partial x\partial y}\right)^2-\frac{\partial^2\bar{w}}{\partial x^2}\frac{\partial^2\bar{w}}{\partial y^2}\right] \tag{9b}$$

Introduce the dimensionless quantities

$$\xi=\frac{x}{a},\quad \eta=\frac{y}{b},\quad w=\frac{\bar{w}}{h},\quad \tau=t\sqrt{\frac{Eh^3}{\rho a^4}},\quad c=v\sqrt{\frac{\rho a^2}{Eh^3}},\quad r=\frac{a}{b},\quad f=\frac{\varphi}{Eh^3},\quad \gamma=\lambda\sqrt{\frac{a^4}{\rho Eh^3}},\quad p=\bar{p}\frac{a^4}{Eh^4},\quad \omega=\bar{\omega}\sqrt{\frac{\rho a^4}{Eh^3}} \tag{10}$$

where γ is the dimensionless damping coefficient.

The dimensionless nonlinear vibration equations of a web with variable density are obtained

$$\left[(1+\alpha)-2\alpha\left|\eta-\frac{1}{2}\right|\right]\left(\frac{\partial^2 w}{\partial\tau^2}+2c\frac{\partial^2 w}{\partial\xi\partial\tau}+c^2\frac{\partial^2 w}{\partial\xi^2}\right)-r^2\frac{\partial^2 f}{\partial\eta^2}\frac{\partial^2 w}{\partial\xi^2}-r^2\frac{\partial^2 f}{\partial\xi^2}\frac{\partial^2 w}{\partial\eta^2}+\gamma\frac{\partial w}{\partial\tau}=p\cos\omega\tau \tag{11a}$$

$$\frac{\partial^4 f}{\partial\xi^4}+r^4\frac{\partial^4 f}{\partial\eta^4}=r^2\left(\frac{\partial^2 w}{\partial\xi\partial\eta}\right)^2-r^2\frac{\partial^2 w}{\partial\xi^2}\frac{\partial^2 w}{\partial\eta^2} \tag{11b}$$

The boundary conditions can be denoted as

$$\begin{cases} w(\xi,0)=0 \\ w(\xi,1)=0 \end{cases} \tag{12}$$

$$\begin{cases} w(0,\eta)=0 \\ w(1,\eta)=0 \end{cases} \tag{13}$$

Separation of the variables

When considering partial differential equations of the nonlinear system, the Bubnov–Galerkin method can be used to separate the time variable and displacement variable. Respectively, they are[31]

$$w(\xi,\eta,\tau)=\sum_{m=1}^{\infty}\sum_{n=1}^{\infty}W_{mn}(\xi,\eta)q_{mn}(\tau) \tag{14}$$

$$f(\xi,\eta,\tau)=\sum_{m=1}^{\infty}\sum_{n=1}^{\infty}F_{mn}(\xi,\eta){q_{mn}}^2(\tau) \tag{15}$$

When $m=n=1$, we obtain

$$w(\xi,\eta,\tau)=W(\xi,\eta)q(\tau) \tag{16}$$

$$f(\xi,\eta,\tau)=F(\xi,\eta)q^2(\tau) \tag{17}$$

Take a displacement function to meet the boundary conditions

$$W(\xi,\eta)=\sin\pi\xi\sin\pi\eta \tag{18}$$

Substituting equations (16)–(18) into equation (11b) yields

$$\frac{\partial^4 F}{\partial\xi^4}+r^4\frac{\partial^4 F}{\partial\eta^4}=\frac{r^2\pi^4}{2}(\cos 2\pi\xi+\cos 2\pi\eta) \tag{19}$$

The solution of equation (19) is obtained

$$F(\xi,\eta)=\frac{r^2}{32}\cos 2\pi\xi+\frac{1}{32r^2}\cos 2\pi\eta \tag{20}$$

Substituting equations (18) and (20) into equation (11a) and adopting the Bubnov–Galerkin method, we obtain

$$\int_0^1\int_0^1\left\{\left[1+\alpha-2\alpha\left|\eta-\frac{1}{2}\right|\right]\left(W\frac{\partial^2 q(\tau)}{\partial\tau^2}+2c\frac{\partial W}{\partial\xi}\frac{\partial q(\tau)}{\partial\tau}+c^2\frac{\partial^2 W}{\partial\xi^2}q(\tau)\right)-r^2\frac{\partial^2 F}{\partial\eta^2}\frac{\partial^2 W}{\partial\xi^2}q^3(\tau)-r^2\frac{\partial^2 F}{\partial\xi^2}\frac{\partial^2 W}{\partial\eta^2}q^3(\tau)+W\gamma\frac{\partial q(\tau)}{\partial\tau}-p\cos\omega\tau\right\}W(\xi,\eta)d\xi d\eta=0 \tag{21}$$

The nonlinear vibration ordinary differential equation of the moving web with variable density can be expressed as

$$A\ddot{q}+B\dot{q}+Cq+Dq^3=\bar{P}\cos\omega\tau \tag{22}$$

where

$$A=\int_0^1\int_0^1\left(1+\alpha-2\alpha\left|\eta-\frac{1}{2}\right|\right)W^2d\xi d\eta=\frac{1}{4}+\frac{\alpha}{8}+\frac{\alpha}{2\pi^2} \tag{23}$$

$$B=2c\int_0^1\int_0^1\left(1+\alpha-2\alpha\left|\eta-\frac{1}{2}\right|\right)\frac{\partial W}{\partial\xi}Wd\xi d\eta+\gamma\int_0^1\int_0^1W^2d\xi d\eta=\frac{\gamma}{4} \tag{24}$$

$$C=c^2\int_0^1\int_0^1\left(1+\alpha-2\alpha\left|\eta-\frac{1}{2}\right|\right)\frac{\partial^2 W}{\partial\xi^2}Wd\xi d\eta=-\pi^2c^2\left(\frac{1}{4}+\frac{\alpha}{8}+\frac{\alpha}{2\pi^2}\right) \tag{25}$$

$$D=-r^2\int_0^1\int_0^1\left(\frac{\partial^2 F}{\partial\eta^2}\frac{\partial^2 W}{\partial\xi^2}+\frac{\partial^2 F}{\partial\xi^2}\frac{\partial^2 W}{\partial\eta^2}\right)Wd\xi d\eta=\frac{\pi^4}{64}(1+r^4) \tag{26}$$

$$\bar{P}=p\int_0^1\int_0^1Wd\xi d\eta=\frac{4}{\pi^2}p \tag{27}$$

The parameter variables are introduced

$$X_1=q,\quad X_2=\dot{X}_1 \tag{28}$$

The state equation of the system is

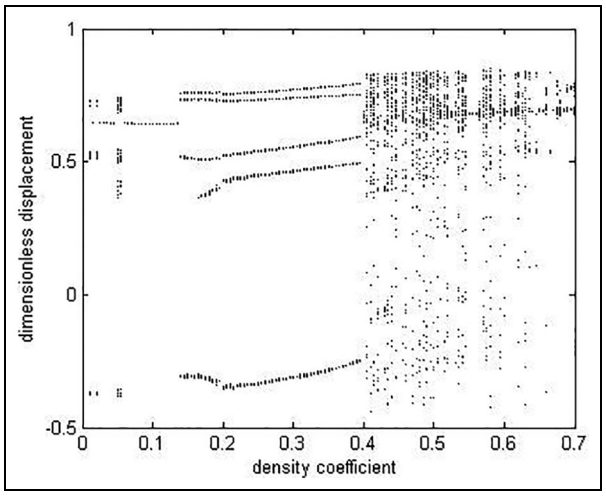

Figure 3. Displacement bifurcation graph of density coefficient ($\omega = 1$, $\gamma = 0.1$, $r = 1$, $c = 0.3$, $p = 0.4$, initial value is (0.01, 0)).

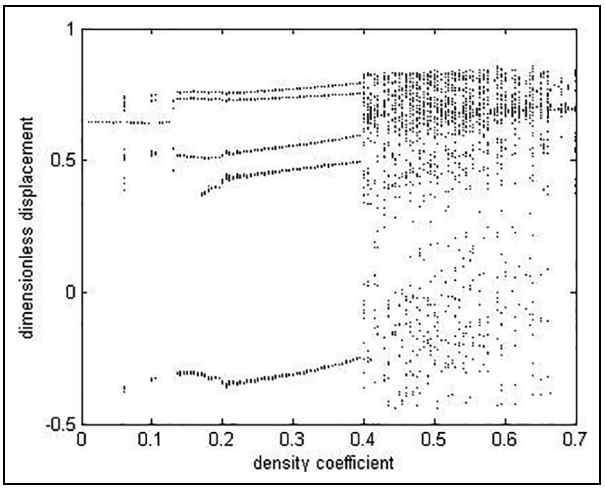

Figure 4. Displacement bifurcation graph of density coefficient ($\omega = 1$, $\gamma = 0.1$, $r = 1$, $c = 0.3$, $p = 0.4$, initial value is (0.001, 0)).

$$\dot{X}_2 = -\frac{2\pi^2\gamma}{2\pi^2 + \alpha\pi^2 + 4\alpha}X_2 + \pi^2 c^2 X_1 - \frac{\pi^6}{16\pi^2 + 8\pi^2\alpha + 32\alpha}(1 + r^4)X_1^3 + \frac{32}{2\pi^2 + \pi^2\alpha + 4\alpha}p\cos\omega\tau \quad (29)$$

Numerical results

The fourth-order Runge–Kutta technique is used to determine the characteristics of nonlinear vibration in a moving printing web. The basic parameters of the printing web are commonly used in the printing.

Effects of density coefficient on nonlinear vibration characteristics

Shown in Figure 3 is the displacement bifurcation graph of density coefficient; when the non-dimensional excitation frequency ω is 1, external excitation amplitude p is 0.4, dimensionless damping coefficient γ is equal to 0.1, dimensionless speed c is 0.3, and aspect ratio $r = 1$, (0.01, 0) is taken as the initial value and the range of density coefficient is $0.01 \leqslant \alpha \leqslant 0.7$. Figure 3 shows that when $0.01 \leqslant \alpha < 0.405$, $0.545 < \alpha < 0.57$, and $0.635 < \alpha \leqslant 0.7$, the bifurcation graph further illustrates that in these regions, the web is in a state of periodic motion, and the web is stable. When $0.405 \leqslant \alpha \leqslant 0.545$ and $0.57 \leqslant \alpha \leqslant 0.635$, the bifurcation graph shows a stack of closely packed dense points, it is shown that the web is in chaotic motion, and therefore, the web is divergence instability in these regions. As a result, the density coefficient increases, the divergence and instability tend to occur easily, and the nonlinear effects increase.

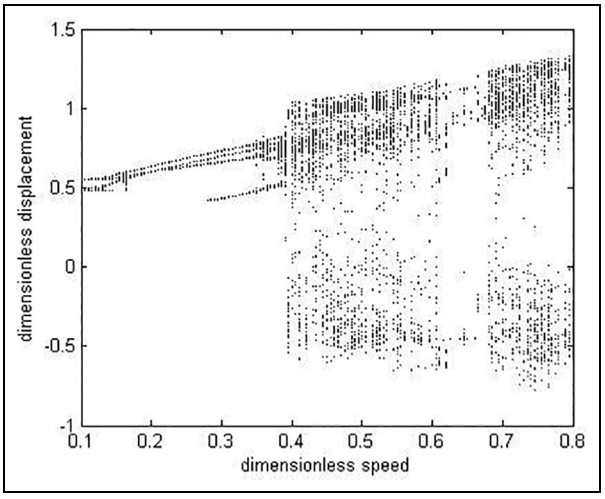

Figure 5. Displacement bifurcation graph of speed ($\omega = 1$, $\gamma = 0.1$, $r = 1$, $\alpha = 0.2$, $p = 1$).

Figure 4 shows the bifurcation diagram of density coefficient and displacement when the initial value is (0.001, 0). As can be seen from Figures 3 and 4, the system motion process is significantly different due to the different initial values. It indicates that the nonlinear vibration of the membrane is sensitive to the initial conditions.

Effects of speed on nonlinear vibration characteristics

As illustrated in Figure 5, for the displacement bifurcation graph of dimensionless speed, when $\gamma = 0.1$, $r = 1$, $\omega = 1$, $\alpha = 0.2$, and $p = 1$, (0.01, 0) is taken as the initial value and the span of dimensionless speed is $0.1 \leqslant c \leqslant 0.8$. Figure 5 illustrates that when $0.1 \leqslant c \leqslant 0.39$ and $0.62 < c < 0.675$, the bifurcation

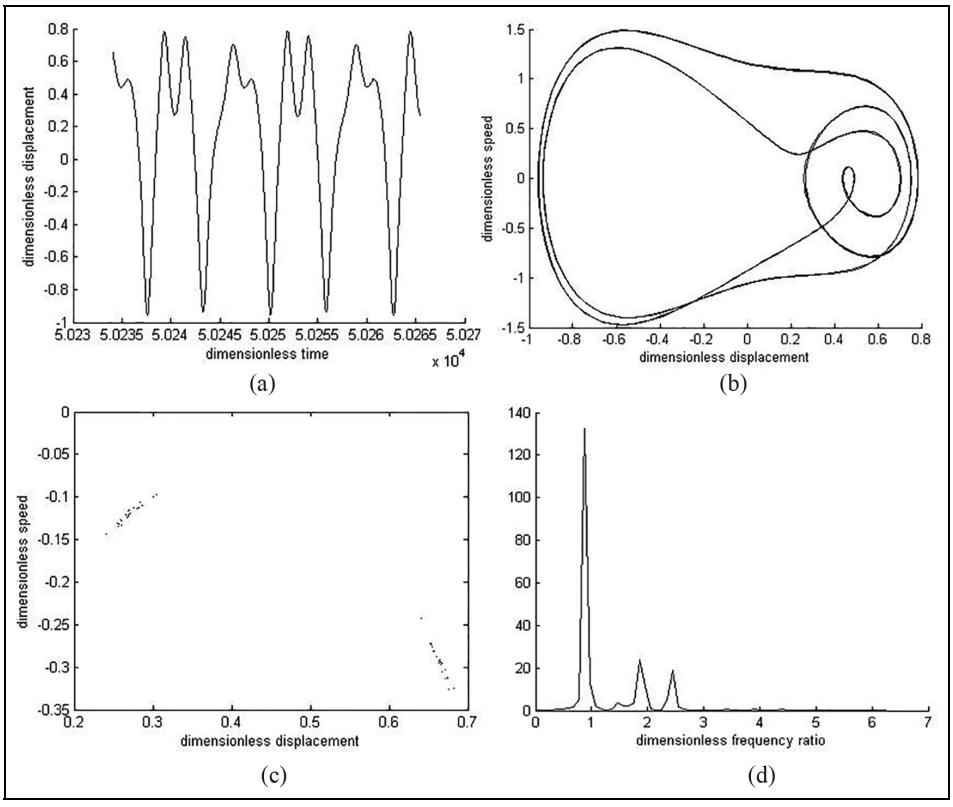

Figure 6. Time histories, phase-plane diagrams, Poincare maps, and power spectrum ($\omega = 1$, $\gamma = 0.1$, $r = 1$, $\alpha = 0.2$, $p = 1$, $c = 0.36$).

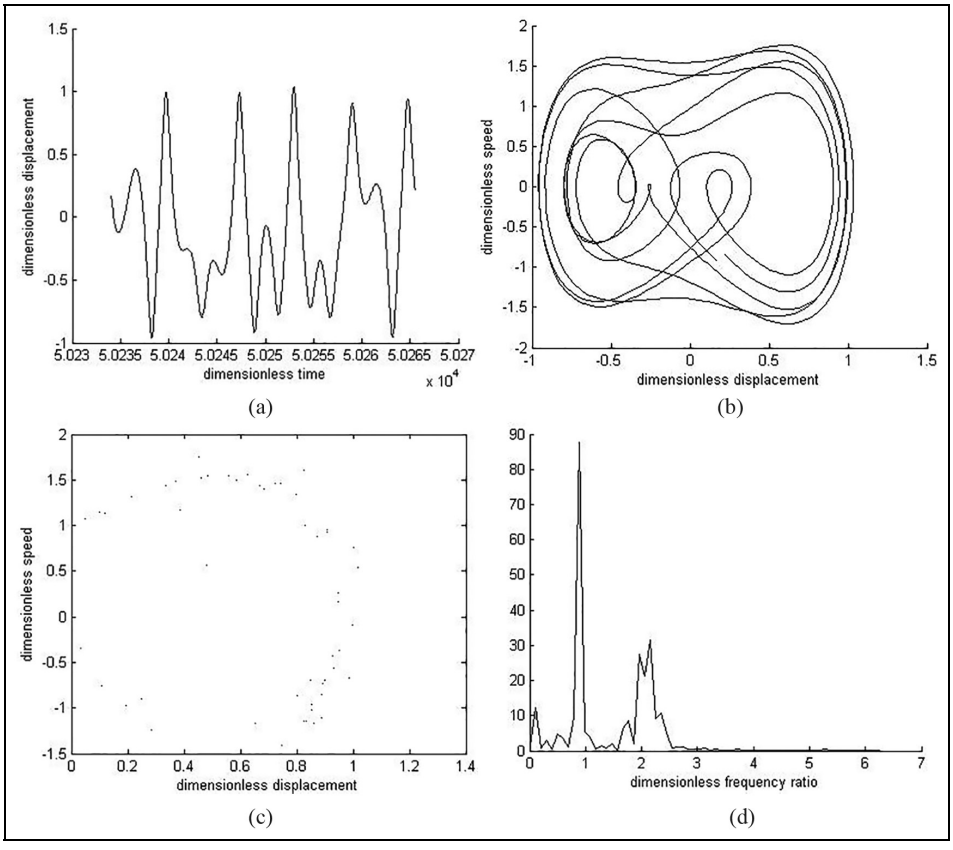

Figure 7. Time histories, phase-plane diagrams, Poincare maps, and power spectrum ($\omega = 1$, $\gamma = 0.1$, $r = 1$, $\alpha = 0.2$, $p = 1$, $c = 0.42$).

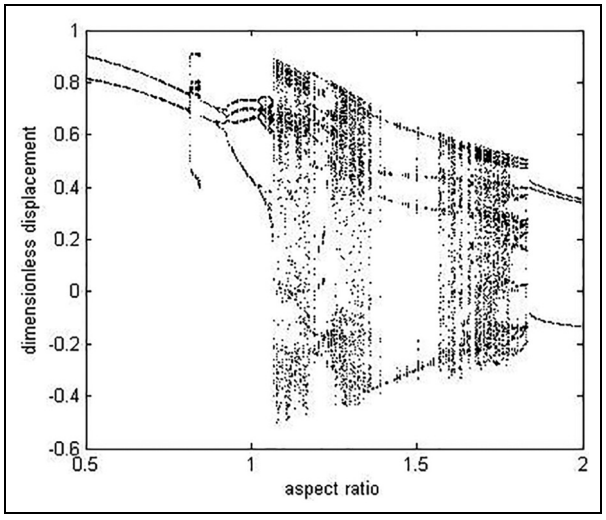

Figure 8. Aspect ratio and displacement bifurcation graph ($\omega = 1$, $\gamma = 0.1$, $c = 0.3$, $\alpha = 0.2$, $p = 1$).

graph shows only a few points, which implies the web is in a state of periodic motion, and it is stable. When $0.39 < c \leqslant 0.62$ and $0.675 < c \leqslant 0.8$, the bifurcation graph shows the irregular dense points, it is shown that the paper web is in chaotic motion, and the web is divergence instability in these regions. As a result, the nonlinear effects increase with the increase in the dimensionless speed. Therefore, we should make a reasonable choice of the printing speed to avoid chaotic motion in the printing process. Overall, the system first from periodic motion transforms into chaotic motion, then enters periodic motion, and finally enters chaos motion completely.

Figures 6 and 7 show the time histories, phase-plane diagrams, Poincare maps, and power spectrum under different dimensionless speeds when $c = 0.36$ and $c = 0.42$, respectively.

As seen in Figures 6 and 7, when $c = 0.36$, it has a large number of regular closed graphics in the phase-plane diagrams, the Poincare maps contain a few discrete points, and power spectrum is discrete, so the system is in multiple periodic motion. When $c = 0.42$, the phase-plane diagram is not closed, the Poincare map contains a lot of dense points, and power spectrum is continuous, so the system is in chaotic motion.

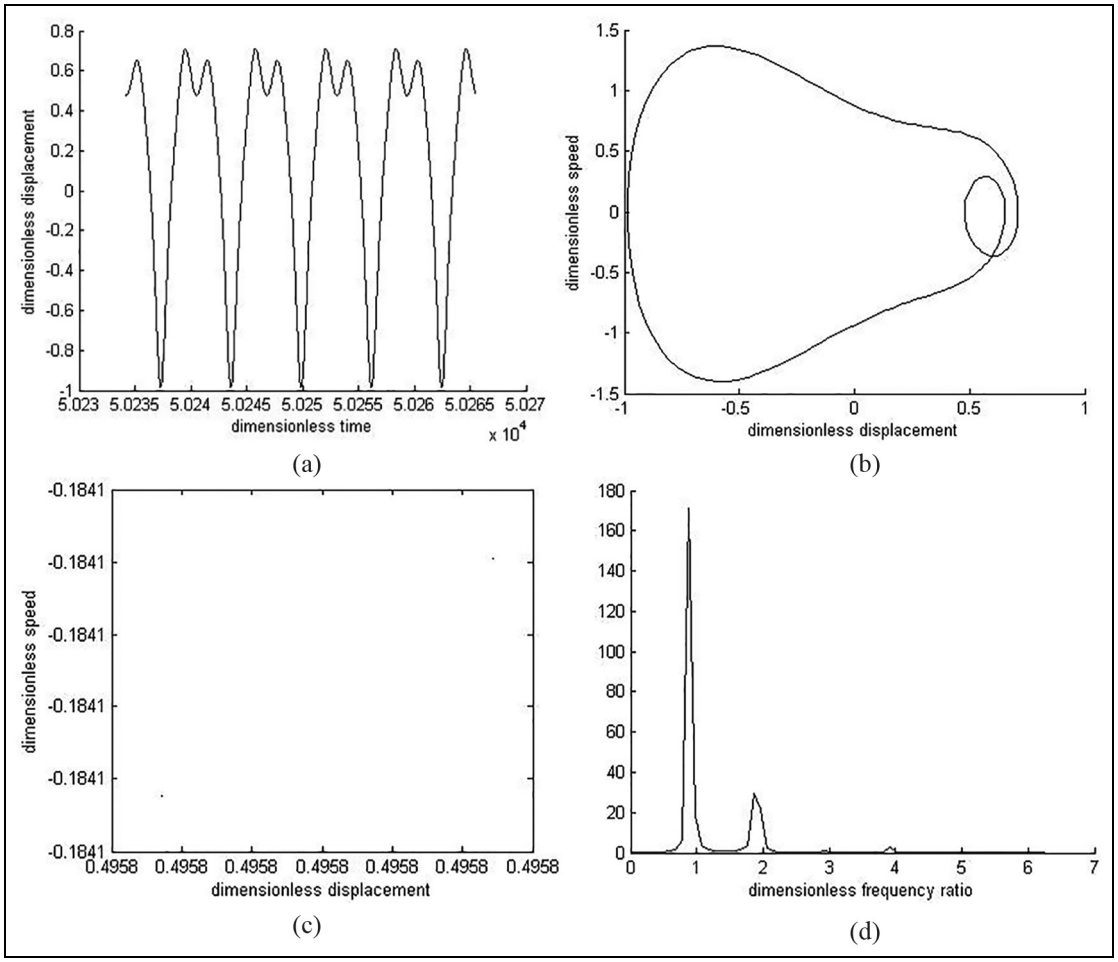

Figure 9. Time histories, phase-plane diagrams, Poincare maps, and power spectrum ($\omega = 1$, $\gamma = 0.1$, $\alpha = 0.2$, $p = 1$, $c = 0.3$, $r = 0.88$).

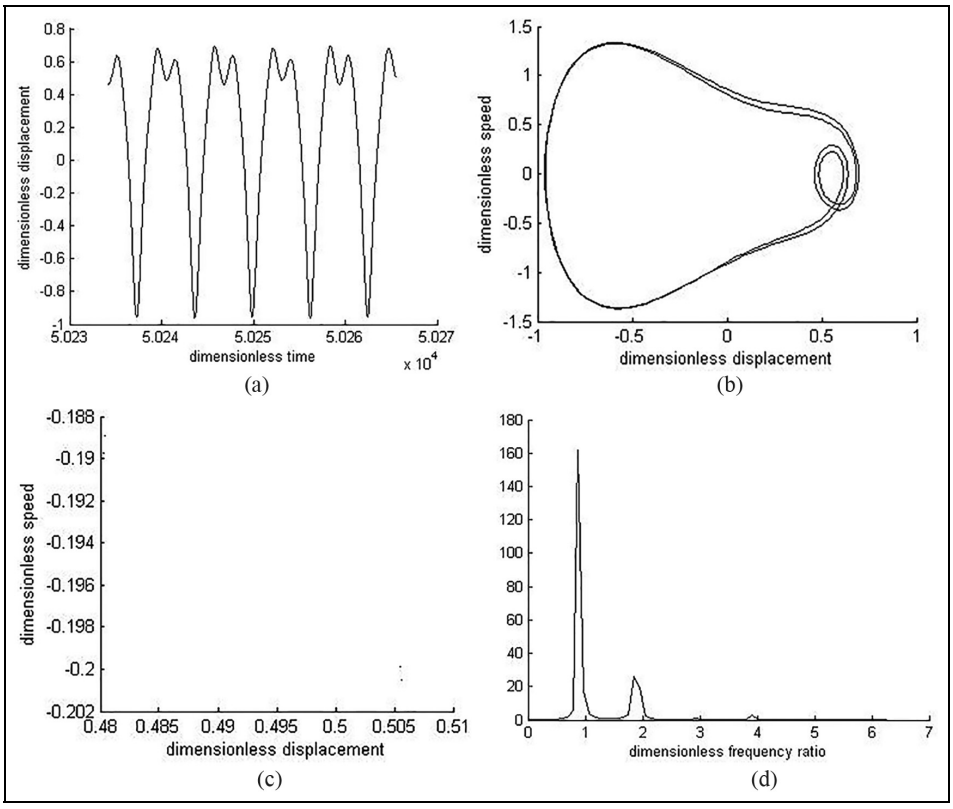

Figure 10. Time histories, phase-plane diagrams, Poincare maps, and power spectrum ($\omega = 1$, $\gamma = 0.1$, $\alpha = 0.2$, $p = 1$, $c = 0.3$, $r = 0.9$).

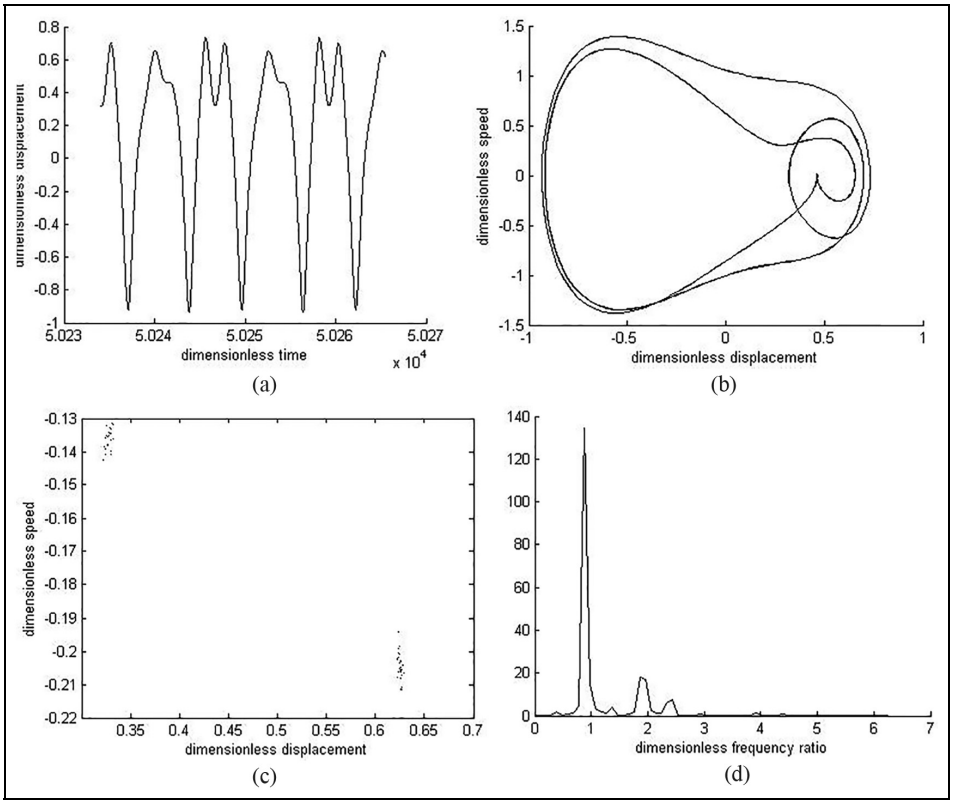

Figure 11. Time histories, phase-plane diagrams, Poincare maps, and power spectrum ($\omega = 1$, $\gamma = 0.1$, $\alpha = 0.2$, $p = 1$, $c = 0.3$, $r = 0.98$).

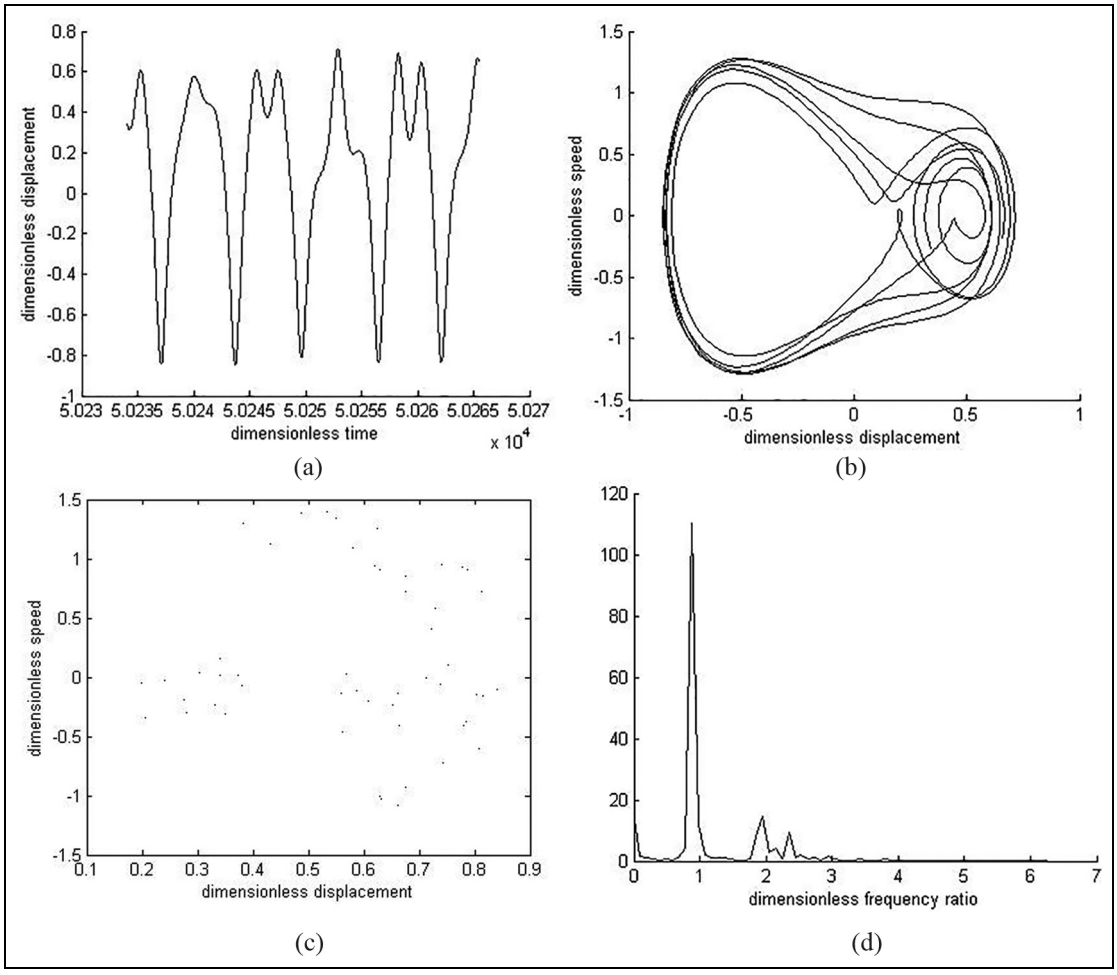

Figure 12. Time histories, phase-plane diagrams, Poincare maps, and power spectrum ($\omega = 1$, $\gamma = 0.1$, $\alpha = 0.2$, $p = 1$, $c = 0.3$, $r = 1.1$).

Effects of aspect ratio on stability

As shown in Figure 8, for the displacement bifurcation graph of aspect ratio, when $\omega = 1$, $\gamma = 0.1$, $c = 0.3$, $\alpha = 0.2$, and $p = 1$, (0.01, 0) is taken as the initial value and $0.5 \leqslant r \leqslant 2$. Figure 8 shows that when $0.5 \leqslant r < 1.07$, $1.36 < r < 1.39$, $1.39 < r < 1.5$, $1.5 < r < 1.57$, and $1.835 < r \leqslant 2$, the bifurcation graph resembles to fewer points; it is specified that membrane is in stable motion in these regions. When $1.07 \leqslant r \leqslant 1.36$, $r = 1.39$, $r = 1.5$, and $1.57 \leqslant r \leqslant 1.835$, the bifurcation graph consists of a stack of dense points, it is shown that the web is in chaotic motion, and the web is divergence instability. It is noted that when the aspect ratio increases, the periodic motion and the chaotic motion exchange alternately.

Figures 9–12 are all about time histories, phase-plane diagrams, Poincare maps, and power spectrum when $r = 0.88$, $r = 0.9$, $r = 0.98$, and $r = 1.1$, correspondingly. It is clear from the figures that the aspect ratio increases gradually, and the system transforms from a state of double periodic motion to quadruple periodic motion, and following this, it enters a state of multiple periodic motion and finally ends up in a state of chaotic motion.

Conclusion

In conclusion, the fourth-order Runge–Kutta technique is employed to analyze the forced nonlinear vibration of a moving paper web with variable density. The effects of the density coefficient, speed, and aspect ratio on the dynamic behavior of a moving paper web are studied. It is evident that

1. When the density coefficient is the control parameter, the web is in a stable working region when the density coefficient is $0.01 \leqslant \alpha < 0.405$, $0.545 < \alpha < 0.57$, and $0.635 < \alpha \leqslant 0.7$. When $0.405 \leqslant \alpha \leqslant 0.545$ and $0.57 \leqslant \alpha \leqslant 0.635$, the web is in an unstable state. As a result, as the density coefficient increases, the divergence and instability tend to occur easily, and the nonlinear effects

increase. Overall, the system has experienced period doubling bifurcation into chaos.

2. When the dimensionless speed is the control parameter, dimensionless speed at the regions $0.1 \leqslant c \leqslant 0.39$ and $0.62 < c < 0.675$ indicates the web is stable. When $0.39 < c \leqslant 0.62$ and $0.675 < c \leqslant 0.8$, the web shows instability. As a result, the nonlinear effects increase when dimensionless speed increases. Overall, the system first undergoes periodic motion and then changes to chaotic motion, and following this, it enters periodic motion again and finally enters chaos motion completely. Therefore, it is important to make a reasonable choice of the printing speed to avoid divergence instability during the printing process.
3. When the aspect ratio is the control parameter, the aspect ratio at these regions is $0.5 \leqslant r < 1.07$, $1.36 < r < 1.39$, $1.39 < r < 1.5$, $1.5 < r < 1.57$, and $1.835 < r \leqslant 2$, and the web is stable. When $1.07 \leqslant r \leqslant 1.36$, $r = 1.39$, $r = 1.5$, and $1.57 \leqslant r \leqslant 1.835$, the web is divergence instability. Therefore, when the aspect ratio increases, the system switches between periodic motion and chaotic motion.

Declaration of conflicting interests

The author(s) declared no potential conflicts of interest with respect to the research, authorship, and/or publication of this article.

Funding

The author(s) disclosed receipt of the following financial support for the research, authorship, and/or publication of this article: This study was supported by the National Natural Science Foundation of China (No. 11272253), the Natural Science Foundation of Shaanxi Province (Nos 2018JM5023, 2018JM1028, 2018JM5119, 2018JM1033), the PhD Innovation fund projects of Xi'an University of Technology (Fund No. 310-252071702), the Central University Special Funds of China (No. 310812171003) and Xi'an Science and Technology Project 2018 (No.201805037YD15CG21(26)).

ORCID iDs

Mingyue Shao https://orcid.org/0000-0003-3889-1999
Jimei Wu https://orcid.org/0000-0002-4695-1376

References

1. Jiang XS, Li CW and Zhang LQ. *Printed materials and suitability*. Harbin, China: Northeast Forestry University press, 2010.
2. Mote CD. On the non-linear oscillation of an axially moving string. *ASME J Appl Mech* 1966; 33: 463–464.
3. Wickert JA and Mote CD. Travelling load response of an axially moving string. *J Sound Vib* 1991; 149: 267–284.
4. Pakdemirli M, Ulsoy AG and Ceranoglu A. Transverse vibration of an axially accelerating string. *J Sound Vib* 1994; 169: 179–196.
5. Chen LQ, Zhang NH and Zu JW. The regular and chaotic vibrations of an axially moving viscoelastic string based on fourth order Galerkin truncation. *J Sound Vib* 2003; 261: 764–773.
6. Chen LQ, Zhang W and Zu JW. Nonlinear dynamics for transverse motion of axially moving strings. *Chaos Soliton Fract* 2009; 40: 78–90.
7. Chen LQ, Tang YQ and Zu JW. Nonlinear transverse vibration of axially accelerating strings with exact internal resonances and longitudinally varying tensions. *Nonlin Dynam* 2014; 76: 1443–1468.
8. Kesimli A, Özkaya E and Bağdatli SM. Nonlinear vibrations of spring-supported axially moving string. *Nonlin Dynam* 2015; 81: 1523–1534.
9. Pellicano F and Vestroni F. Nonlinear dynamics and bifurcations of an axially moving beams. *J Vib Acoust* 2000; 122: 21–30.
10. Öz HR, Pakdemirli M and Boyacı H. Non-linear vibrations and stability of an axially moving beam with time-dependent velocity. *Int J Nonlin Mech* 2001; 36: 107–115.
11. Ghayesh MH. Stability and bifurcations of an axially moving beam with an intermediate spring support. *Nonlin Dynam* 2012; 69: 193–210.
12. Ghayesh MH and Amabili M. Nonlinear vibrations and stability of an axially moving Timoshenko beam with an intermediate spring support. *Mech Mach Theory* 2013; 67: 1–16.
13. Ghayesh MH and Amabili M. Steady-state transverse response of an axially moving beam with time-dependent axial speed. *Int J Nonlin Mech* 2013; 49: 40–49.
14. Tang YQ, Zhang DB and Gao JM. Parametric and internal resonance of axially accelerating viscoelastic beams with the recognition of longitudinally varying tensions. *Nonlin Dynam* 2016; 83: 401–418.
15. Yang XD, Zhang W, Chen LQ, et al. Dynamical analysis of axially moving plate by finite difference method. *Nonlin Dynam* 2012; 67: 997–1006.
16. Wang Y, Tian Z, Wu JM, et al. Dynamic stability of an axially moving paper board with added subsystems. *J Low Freq Noise Vib Act Control* 2018; 37: 48–59.
17. Wang YQ and Zu JW. Vibration behaviors of functionally graded rectangular plates with porosities and moving in thermal environment. *Aerosp Sci Technol* 2017; 69: 550–562.
18. Marynowski K. Non-linear vibrations of the axially moving paper web. *J Theor Appl Mech* 2008; 46: 565–580.
19. Marynowski K. Non-linear vibrations of an axially moving viscoelastic web with time-dependent tension. *Chaos Soliton Fract* 2004; 21: 481–490.
20. Lin CC and Mote CD. Equilibrium displacement and stress distribution in a two-dimensional, axially moving web under transverse loading. *J Appl Mech* 1995; 62: 772–779.
21. Zhao FQ and Wang ZM. Nonlinear vibration analysis of a moving rectangular membrane. *Mech Sci Technol Aerosp Eng* 2010; 29: 768–771 (in Chinese).
22. Soares RM and Gonçalves PB. Nonlinear vibrations and instabilities of a stretched hyperelastic annular membrane. *Int J Solid Struct* 2012; 49: 514–526.

23. Gajbhiye SC, Upadhyay SH and Harsha SP. Nonlinear vibration analysis of piezo-actuated flat thin membrane. *J Vib Control* 2013; 21: 1162–1170.
24. Li D, Zheng ZL, Tian Y, et al. Stochastic nonlinear vibration and reliability of orthotropic membrane structure under impact load. *Thin Wall Struct* 2017; 119: 247–255.
25. Jabareen M and Eisenberger M. Free vibrations of non-homogeneous circular and annular membranes. *J Sound Vib* 2001; 240: 409–429.
26. Subrahmanyam PB and Sujith RI. Exact solutions for axisymmetric vibrations of solid circular and annular membranes with continuously varying density. *J Sound Vib* 2001; 248: 371–378.
27. Willatzen M. Exact power series solutions for axisymmetric vibrations of circular and annular membranes with continuously varying density in the general case. *J Sound Vib* 2002; 258: 981–986.
28. Ma LE, Wu JM, Mei XS, et al. Active vibration control of moving web with varying density. *J Low Freq Noise Vib Act Control* 2013; 32: 323–334.
29. Buchanan GR. Vibration of circular membranes with linearly varying density along a diameter. *J Sound Vib* 2005; 280: 407–414.
30. Xu ZL. *Elastic mechanics part II*. Beijing, China: Higher Education Press, 2015.
31. Liu CJ, Zheng ZL and Yang XY. Analytical and numerical studies on the nonlinear dynamic response of orthotropic membranes under impact load. *Earthq Eng Eng Vib* 2016; 15: 657–672.